SEMARAK ILMU PUBLISHING

Journal of Advanced Research in Fluid Mechanics and Thermal Sciences

Journal homepage:
https://semarakilmu.com.my/journals/index.php/fluid_mechanics_thermal_sciences/index
ISSN: 2289-7879

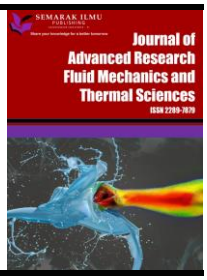

A Critical Review of All Mathematical Models Developed for Solar Air Heater Analysis

Doan Thi Hong Hai[1], Nguyen Minh Phu[1,*]

[1] Faculty of Heat and Refrigeration Engineering, Industrial University of Ho Chi Minh City (IUH), Vietnam

ARTICLE INFO

Article history:
Received 30 November 2022
Received in revised form 12 March 2023
Accepted 20 March 2023
Available online 6 April 2023

Keywords:
Stationary model; lumped model; transient model; dynamic model; solar air heater

ABSTRACT

In this paper, three mathematical models to predict the air collector temperature are reviewed and analyzed. These three models were drawn from 30 publications between 1980 and 2022. The models include lumped model (model 1), a one-dimensional (1D) steady model (model 2), and 1D unsteady model (model 3). The models are established based on the energy balance of the heat exchanger surfaces and the airflow. Solution techniques for models are presented using a system of linear equations, numerical integral, and finite difference method. The results of the sensitivity analysis of the models indicate that the temperatures of the air exiting the collector are similar. Model 3 considers the thickness of the glass cover, absorber plate, and bottom plate thus having the effect of thermal inertia in the morning and afternoon. The maximum difference of outlet air temperature between models 1 and 2 is 0.18 K. The highest outlet air temperature deviation of 0.77 K between models 1 and 3 occurred at 8 AM. When the thicknesses are negligible, the temperature distribution along the air collector of models 2 and 3 is the same. In other words, model 3 should be used when there is the presence of the thickness of the plates and the glass cover.

1. Introduction

Solar air heater (SAH) is a device that converts energy from solar irradiance into hot air. This converter is widely applied in drying technology [1,2], ventilation, and space heating [3]. It has a simple structure and is easy to manufacture. However, the efficiency is low because the heat transfer fluid is air [4,5]. It has therefore received enormous research attention in the past half-century. Recently, nanopowders have been inserted to the heat transfer fluid to improve the thermohydraulic performance of a thermal solar system [6-8]. The SAH has been studied scholarly since 1963 [9]. Scopus data indicates that there are more than 4000 published articles related to solar air heater research. Figure 1 shows the number of SAH papers in the last 5 years. An increasing trend can be seen in research on SAH. The mathematical model for the thermal design of the air collector can be divided into three categories according to the complexity of the mathematical problem as follows

* *Corresponding author.*
E-mail address: nguyenminhphu@iuh.edu.vn

https://doi.org/10.37934/arfmts.105.1.114

i. Model 1: Lumped model
ii. Model 2: One-dimensional (1D) steady model
iii. Model 3: 1D unsteady model

Model 1 is the steady-state lumped parameters model. The temperatures of the air collector components (glass, airflow, absorber plate, bottom plate) are average temperatures. This is the simplest mathematical approach. Model 2 considers the variation of air temperature along the flow direction so that it forms an ordinary differential equation (ODE) or an air temperature gradient equation. Model 3 is derived from the differential equation of energy, i.e., second-order partial differential equation (PDE). Therefore, model 3 is the most complicated and often solved using a numerical method. It should be noted that multi-dimensional (2D or 3D) and unsteady models weren't analytically performed. This is because of involvement of pressure-velocity and non-linear term in Navier-Stokes equation which is so complicated that such an approach is unnecessary.

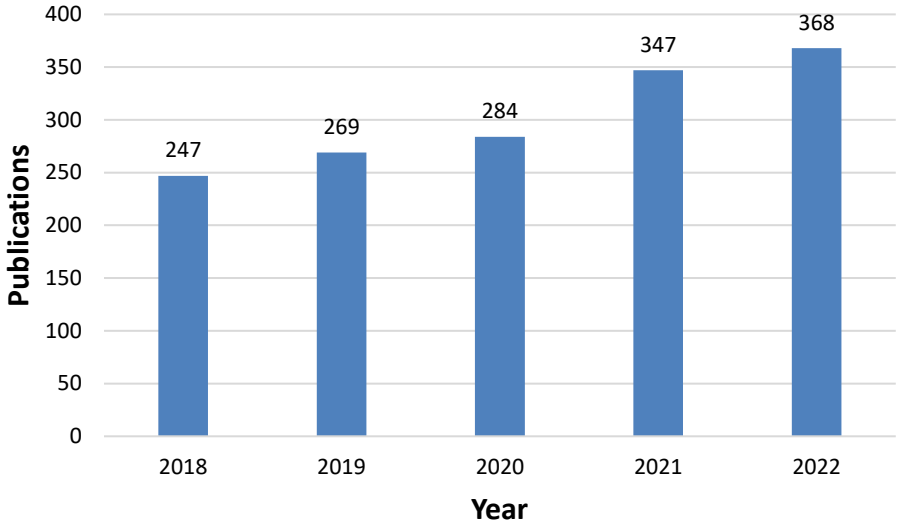

Fig. 1. Number of publications titled "solar air heater" in recent five years (Source: Scopus database)

Table 1 summarizes the analytical publications on solar air heaters from the year 1980. Apart from a specific application, the mathematical formulation of a publication is one of the three models aforementioned above. Most researchers have used the first two approaches due to their simplicity. Recently, Román and Hensel [10] have confirmed that few studies have employed the model 3 in the study of solar air collectors. Actually, there is not a work which points out strengths, weaknesses, and comparison of the three models. The analysis of mathematical approaches is very important for designers in calculation of a thermal solar system. They can select either simplified model with moderate accuracy or well-established model with high enough skills of advanced calculus and numerical method. Therefore, the aim of this study is to

i. Overview the mathematical models for the thermal design of the air collector (as shown in Table 1)
ii. Establish three analytical approaches and discuss solution procedure.
iii. Compare the outlet air temperature and local temperatures of the approaches.

Table 1
Summary of the research work on solar air collectors using an analytical approach

No.	Year	Researcher	Model1 (lumped)	Model 2 (ODE)	Model3 (PDEs)
1	1980	El-Refaie and Hashish [5]			✓
2	1981	Garg *et al.,* [6]			✓
3	1989	Garg *et al.,* [7]			✓
4	1995	Ong [8]	✓	✓	
5	2005	Ho *et al.,* [9]		✓	
6	2007	Ramadan *et al.,* [10]		✓	
7	2009	Sopian *et al.,* [11]			✓
8	2010	Ramani *et al.,* [12]		✓	
9	2013	Yeh and Ho [13]		✓	
10	2013	Hernandez and Quiñonez [14]		✓	
11	2013	Ho *et al.,* [15]		✓	
12	2014	Karim *et al.,* [16]	✓		
13	2015	Velmurugan and Kalaivanan [17]	✓		
14	2015	Velmurugan and Kalaivanan [18]	✓		
15	2015	Velmurugan and Kalaivanan [19]	✓		
16	2016	Velmurugan and Kalaivanan [20]	✓		
17	2018	Singh and Dhiman [21]		✓	
18	2018	Ho *et al.,* [22]		✓	
19	2018	Matheswaran *et al.,* [23]	✓		
20	2019	Matheswaran *et al.,* [24]	✓		
21	2021	Luan and Phu [25]	✓		
22	2021	Phu *et al.,* [26]		✓	
23	2021	Phu and Tu [27]		✓	
24	2021	Phu *et al.,* [28]		✓	
25	2021	Ahmadkhani *et al.,* [29]		✓	
26	2021	Ho *et al.,* [30]		✓	
27	2022	Phu and Hap [31]	✓	✓	
28	2022	Nhiem *et al.,* [32]		✓	
29	2022	Thao *et al.,* [33]		✓	
30	2022	Román and Hensel [4]			✓

2. Mathematical Models

Figure 2 outlines the schematic diagram of a single-pass flat plate solar air heater used for mathematical modeling and analysis in this study. Solar radiation (I) passes through the glass cover and solar energy is absorbed by the absorber plate. The air flow blows below the absorber plate to receive heat from the absorber and bottom plates. The lower side of the bottom plate is thermally insulated to reduce heat loss. Movement of the air between the glass and the absorber plate is considered natural convection. The collector has length L, width W, and air channel height H. Air enters the collector at temperature T_a, velocity V, and exits the collector at temperature T_o. The convection heat transfer coefficients (h_c and h_{nc}) and the radiation heat transfer coefficients (h_r) are also denoted in the figure. Different approaches to estimate collector temperature are presented in sub-sessions.

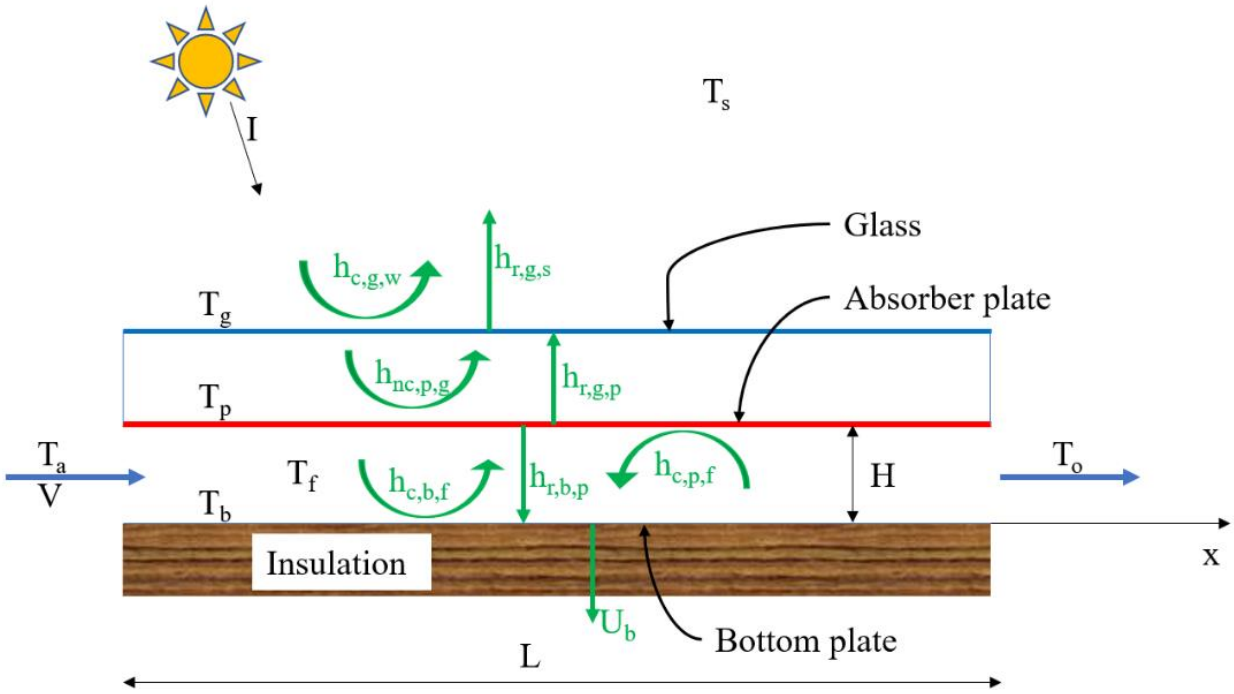

Fig. 2. Sketch of single-pass flat plate solar air heater

2.1 Mean Temperature Model (Lumped Model)

In this model, the glass temperature (T_g), the absorber plate temperature (T_p), the air temperature (T_f), and the bottom plate temperature (T_b) are the average temperatures at the time being considered. The temperatures are calculated from the energy balance equation as follows. The amount of heat that the glass receives from solar energy is balanced with thermal convection on the glass surface with wind, natural convection between the glass and the absorber, radiation between these two surfaces, and radiation between the glass and the sky [31]

$$0 = I\alpha_g + h_{c,g,w}(T_a - T_g) + h_{nc,p,g}(T_p - T_g) + h_{r,g,p}(T_p - T_g) + h_{r,g,s}(T_s - T_g) \quad (1)$$

where T_s is the sky temperature, $T_s = 0{,}0552T_a^{1.5}$ [14], other symbols can be seen in sub-session 2.4 and Table 2.

The absorber plate heat received from solar energy is balanced with the heat generated by convection between the glass and the air current, natural convection between the air and the absorber plate, radiation between the glass and the plate, and radiation between the plates

$$0 = I\alpha_p\tau_g + h_{c,p,f}(T_f - T_p) + h_{r,g,p}(T_g - T_p) + h_{nc,p,g}(T_g - T_p) + h_{r,b,p}(T_b - T_p) \quad (2)$$

The heat received by the air through the collector is equal to the heat due to convection of the airflow with the bottom plate and the absorber plate

$$Hc_{p,f}\rho_f V\frac{T_a - T_o}{L} = h_{c,b,f}(T_b - T_f) + h_{c,p,f}(T_p - T_f) \quad (3)$$

where $T_f = \frac{T_a + T_o}{2}$

The convective heat exchange between the bottom plate and the air stream, the thermal radiation between the plates and the heat loss through the insulation are balanced as follows

$$0 = \mathrm{h}_{\mathrm{c,b,f}}(\mathrm{T_f} - \mathrm{T}_b) + \mathrm{h}_{\mathrm{r,b,p}}(\mathrm{T}_p - \mathrm{T}_b) + U_b(T_a - T_b) \tag{4}$$

2.2 One-Dimensional (1D) Steady Model (ODE)

In this approach, the temperatures of T_g, T_p, T_f, and T_b vary with direction of airflow at the time being evaluated, i.e., T = T(x). The formulation is the same as the former except the air temperature difference in Eq. (3) transformed to the differential air temperature (see Eq. (7)) [14]

$$0 = I\alpha_g + h_{c,g,\mathrm{w}}(\mathrm{T_a} - \mathrm{T_g}) + \mathrm{h}_{\mathrm{nc,p,g}}(\mathrm{T}_p - \mathrm{T}_g) + \mathrm{h}_{\mathrm{r,g,p}}(\mathrm{T_p} - \mathrm{T_g}) + h_{r,g,s}(T_s - T_g) \tag{5}$$

$$0 = I\alpha_p\tau_g + \mathrm{h}_{\mathrm{c,p,f}}(\mathrm{T_f} - \mathrm{T}_p) + \mathrm{h}_{\mathrm{r,g,p}}(\mathrm{T}_g - \mathrm{T}_p) + \mathrm{h}_{\mathrm{nc,p,g}}(\mathrm{T}_g - \mathrm{T}_p) + \mathrm{h}_{\mathrm{r,b,p}}(\mathrm{T}_b - \mathrm{T}_p) \tag{6}$$

$$Hc_{p,\mathrm{f}}\rho_f V\frac{dT_f}{dx} = \mathrm{h}_{\mathrm{c,b,f}}(\mathrm{T}_b - \mathrm{T}_f) + \mathrm{h}_{\mathrm{c,p,f}}(\mathrm{T_p} - \mathrm{T}_f) \tag{7}$$

$$0 = \mathrm{h}_{\mathrm{c,b,f}}(\mathrm{T_f} - \mathrm{T}_b) + \mathrm{h}_{\mathrm{r,b,p}}(\mathrm{T}_p - \mathrm{T}_b) + U_b(T_a - T_b) \tag{8}$$

Boundary condition for Eq. (7): $T_f|_{x=0} = T_a$.

2.3 One-Dimensional (1D) Unsteady Model (PDEs)

In this modeling, the temperatures of T_g, T_p, T_f, and T_b change with direction of airflow and time, i.e., T = T(x, t). In this regard, energy balance equation for each component was derived from the unsteady convection–diffusion equation [12]

$$\delta_g c_{p,g}\rho_g\frac{\partial T_g}{\partial t} = k_g\delta_g\frac{\partial^2 T_g}{\partial x^2} + I\alpha_g + h_{c,g,\mathrm{w}}(\mathrm{T_a} - \mathrm{T_g}) + \mathrm{h}_{\mathrm{nc,p,g}}(\mathrm{T}_p - \mathrm{T}_g) + \mathrm{h}_{\mathrm{r,g,p}}(\mathrm{T_p} - \mathrm{T_g}) + h_{r,g,s}(T_s - T_g) \tag{9}$$

$$\delta_p c_{p,p}\rho_p\frac{\partial T_p}{\partial t} = k_p\delta_p\frac{\partial^2 T_p}{\partial x^2} + I\alpha_p\tau_g + \mathrm{h}_{\mathrm{c,p,f}}(\mathrm{T_f} - \mathrm{T}_p) + \mathrm{h}_{\mathrm{r,g,p}}(\mathrm{T}_g - \mathrm{T}_p) + \mathrm{h}_{\mathrm{nc,p,g}}(\mathrm{T}_g - \mathrm{T}_p) + \mathrm{h}_{\mathrm{r,b,p}}(\mathrm{T}_b - \mathrm{T}_p) \tag{10}$$

$$Hc_{p,\mathrm{f}}\rho_f\frac{\partial T_f}{\partial t} + Hc_{p,\mathrm{f}}\rho_f V\frac{\partial T_f}{\partial x} = k_f H\frac{\partial^2 T_f}{\partial x^2} + \mathrm{h}_{\mathrm{c,b,f}}(\mathrm{T}_b - \mathrm{T}_f) + \mathrm{h}_{\mathrm{c,p,f}}(\mathrm{T_p} - \mathrm{T}_f) \tag{11}$$

$$\delta_b c_{p,\mathrm{b}}\rho_b\frac{\partial T_b}{\partial t} = k_b\delta_b\frac{\partial^2 T_b}{\partial x^2} + \mathrm{h}_{\mathrm{c,b,f}}(\mathrm{T_f} - \mathrm{T}_b) + \mathrm{h}_{\mathrm{r,b,p}}(\mathrm{T}_p - \mathrm{T}_b) + U_b(T_a - T_b) \tag{12}$$

Boundary conditions

$$T_f|_{x=0} = T_a, \tag{13}$$

$$\left.\frac{\partial T_f}{\partial x}\right|_{x=L} = 0, \tag{14}$$

$$\left.\frac{\partial T_g}{\partial x}\right|_{x=0} = \left.\frac{\partial T_g}{\partial x}\right|_{x=L} = 0, \tag{15}$$

$$\left.\frac{\partial T_p}{\partial x}\right|_{x=0} = \left.\frac{\partial T_p}{\partial x}\right|_{x=L} = 0, \tag{16}$$

$$\left.\frac{\partial T_b}{\partial x}\right|_{x=0} = \left.\frac{\partial T_b}{\partial x}\right|_{x=L} = 0. \tag{17}$$

Initial conditions of the four temperatures are the air temperature at the start of the simulation.

2.4 Heat Transfer Coefficients

Natural convection heat transfer coefficient between glass and absorber plate [24]

$$\mathrm{h_{nc,p,g}} = 1.25(\mathrm{T}_p - \mathrm{T}_g)^{0.25} \tag{18}$$

Radiant heat transfer coefficient between glass and sky

$$h_{r,g,s} = \sigma\varepsilon_g\left(T_g{}^2 + T_s{}^2\right)\left(T_g + T_s\right) \tag{19}$$

where σ is the Stefan's constant.

Radiant heat transfer coefficient between glass and absorber plate

$$h_{r,g,p} = \sigma\left(T_g{}^2 + T_p{}^2\right)\frac{T_g+T_p}{1/\varepsilon_g+1/\varepsilon_p-1} \tag{20}$$

Radiant heat transfer coefficient between the bottom plate and the absorber plate

$$h_{r,b,p} = \sigma\left(T_b{}^2 + T_p{}^2\right)\frac{T_b+T_p}{1/\varepsilon_b+1/\varepsilon_p-1} \tag{21}$$

The convection heat transfer coefficient between the glass and the ambient wind is calculated according to the McAdam's correlation [14]

$$h_{c,g,w} = 5.7 + 3.8V_w \tag{22}$$

The forced convection heat transfer coefficient between the bottom plate and the airflow, and the forced convective heat transfer coefficient between the absorber plate and the airflow [25]

$$h_{c,b,f} = h_{c,p,f} = 0{,}018Re^{0,8}Pr^{0,4}k_f/D_h \tag{23}$$

where Re and Pr are respectively Reynolds number and Prandtl number of the airflow, D_h is the hydraulic diameter of the air channel.

$$Re = 2\frac{m}{\mu_f(W+H)} \tag{24}$$

where m is the air mass flow rate.

$$m = \rho_f VWH \tag{25}$$

$$D_h = \frac{4HW}{2(H+W)} \tag{26}$$

$$Pr = c_{p,f}\mu_f / k_f \tag{27}$$

The loss coefficient from the bottom plate through the insulation is calculated as follows

$$U_b = k_i / \delta_i \tag{28}$$

3. Solution Techniques

3.1 Mean Temperature Model

Eq. (1)-(4) can be rearranged to the system of linear equations as

$$\begin{bmatrix} S_{11} & -(\mathrm{h}_{\mathrm{nc,p,g}}+\mathrm{h}_{\mathrm{r,p,g}}) & 0 & 0 \\ -(\mathrm{h}_{\mathrm{nc,p,g}}+\mathrm{h}_{\mathrm{r,p,g}}) & S_{22} & -h_{c,p,f} & -h_{r,b,p} \\ 0 & h_{c,p,f} & S_{33} & h_{c,b,f} \\ 0 & -h_{r,b,p} & -h_{c,b,f} & S_{44} \end{bmatrix} \begin{bmatrix} T_g \\ T_p \\ T_f \\ T_b \end{bmatrix} = \begin{bmatrix} S_1 \\ S_2 \\ S_3 \\ S_4 \end{bmatrix} \tag{29}$$

where

$$\begin{aligned} S_{11} &= h_{c,g,w} + h_{nc,p,g} + h_{r,g,p} + h_{r,g,s} \\ S_1 &= I\alpha_g + h_{r,g,s}T_s + h_{c,g,\mathrm{w}}\,\mathrm{T_a} \\ S_{22} &= h_{c,\mathrm{p,f}} + h_{nc,p,g} + h_{r,g,p} + h_{r,\mathrm{b,p}} \\ S_2 &= I\alpha_p\tau_g \\ S_{33} &= 2Hc_{p,f}\rho_f V - h_{c,b,f}L - h_{c,p,f}L \\ S_3 &= 2Hc_{p,f}\rho_f V\,\mathrm{T_a} \\ S_{44} &= h_{c,b,f} + h_{\mathrm{r,b,p}} + U_b \\ S_4 &= U_b\,\mathrm{T_a} \end{aligned} \tag{30}$$

The straightforward system of linear equations (29) can be solved for the temperatures of T_g, T_p, T_f, and T_b once the qualities S are given.

3.2 One-Dimensional Steady Model

To solve ordinary differential equations (Eq. (7)), numerical integration can be applied. Details of the solving sequence can be found in the textbook [40]. In this regard, the Eq. (7) is written in integral form as:

$$T_f = T_a + \int_0^L \frac{dT_f}{dx}dx \tag{31}$$

3.3 One-Dimensional Unsteady Model

The governing equations in this approach can be rewritten by

$$\frac{\partial T_g}{\partial t} = \alpha_g \frac{\partial^2 T_g}{\partial x^2} + S_g \tag{32}$$

$$\frac{\partial T_p}{\partial t} = \alpha_p \frac{\partial^2 T_p}{\partial x^2} + S_p \tag{33}$$

$$\frac{\partial T_f}{\partial t} + V \frac{\partial T_f}{\partial x} = \alpha_f \frac{\partial^2 T_f}{\partial x^2} + S_f \tag{34}$$

$$\frac{\partial T_b}{\partial t} = \alpha_b \frac{\partial^2 T_b}{\partial x^2} + S_b \tag{35}$$

The PDEs (32)-(35) has the common form as Unsteady term + Convection term = Diffusion term + Source term. The PDEs can be unfolded using the finite difference method. The equations discretized by implicit method, central difference for the diffusion term, upwind scheme for convection term is shown in Eq. (36)-(39). To avoid non-linear problem, source terms (S) were calculated in the previous time step [10]. The tri-diagonal matrix algorithm (TDMA) can be used to solve the system of linear equations.

$$\frac{T_{g,i}^{n+1} - T_{g,i}^{n}}{\Delta t} = \alpha_g \frac{T_{g,i+1}^{n+1} - 2T_{g,i}^{n+1} + T_{g,i-1}^{n+1}}{\Delta x^2} + S_g^i \tag{36}$$

$$\frac{T_{p,i}^{n+1} - T_{p,i}^{n}}{\Delta t} = \alpha_p \frac{T_{p,i+1}^{n+1} - 2T_{p,i}^{n+1} + T_{p,i-1}^{n+1}}{\Delta x^2} + S_p^i \tag{37}$$

$$\frac{T_{f,i}^{n+1} - T_{f,i}^{n}}{\Delta t} + V \frac{T_{f,i-1}^{n+1} - T_{f,i}^{n+1}}{\Delta x} = \alpha_f \frac{T_{f,i+1}^{n+1} - 2T_{f,i}^{n+1} + T_{f,i-1}^{n+1}}{\Delta x^2} + S_f^i \tag{38}$$

$$\frac{T_{b,i}^{n+1} - T_{b,i}^{n}}{\Delta t} = \alpha_b \frac{T_{b,i+1}^{n+1} - 2T_{b,i}^{n+1} + T_{b,i-1}^{n+1}}{\Delta x^2} + S_b^i \tag{39}$$

The validation of models 1 and 2 can be seen in our previous studies [31,34]. The results of model 3 will be confirmed with those of models 1 and 2 in the next session.

4. Example

This section presents the numeric results calculated from the models with the same inputs as shown in Table 2. Most parameters were obtained from the study of Román and Hensel [10] as default properties in SAH research. It is noted that the models 1 and 2 do not need the thermo-physical properties and thickness of glass, absorber plate, and bottom plate (c_p, k, ρ, and δ). Hourly solar radiation and ambient temperature were taken from Eq. (40) and (41) [12,41], respectively. They were also plotted in Figure 3(a).

$$\begin{aligned} I = 237.17 &+ 388.7\mathrm{Cos}(w_1 t - 3.272) + 195.8\mathrm{Cos}(2w_1 t - 0.2757) \\ &+ 27.62\mathrm{Cos}(3w_1 t - 3.8) + 38.44\mathrm{Cos}(4w_1 t - 3.44) \\ &+ 17.76\mathrm{Cos}(5w_1 t - 4.536) \end{aligned} \tag{40}$$

$$T_a = 14.354 + 6.11\text{Cos}(w_1 t - 3.858) + 1.88\text{Cos}(2w_1 t - 0.509) + 0.225\text{Cos}(3w_1 t - 1.25) + 0.288\text{Cos}(4w_1 t - 2.62) + 0.146\text{Cos}(5w_1 t - 3.92) \quad (41)$$

where $w_1 = \frac{\pi}{12}\ rad/h$

Table 2
Input parameters

Parameter	Symbol	Value
Specific heat of air	$c_{p,f}$	1005 J/kg.K
Conductivity of air	k_f	0.02588 W/m.K
Density of air	ρ_f	1.164 kg/m^3
Viscosity of air	μ_f	1.983e-5 Pa.s
Specific heat of glass	$c_{p,g}$	666 J/kg.K
Conductivity of glass	k_g	1.05 W/m.K
Density of glass	ρ_g	2500 kg/m^3
Thickness of glass	δ_g	3 mm
Absorptance, transmittance, emissivity of glass	α_g, τ_g, ε_g	0.06, 0.84, 0.9
Specific heat of absorber plate	$c_{p,p}$	903 J/kg.K
Conductivity of absorber plate	k_p	237 W/m.K
Density of absorber plate	ρ_p	2700 kg/m^3
Thickness of absorber plate	δ_p	1 mm
Absorptance, emissivity of absorber plate	α_p, ε_p	0.95, 0.95
Specific heat of bottom plate	$c_{p,b}$	903 J/kg.K
Conductivity of bottom plate	k_b	237 W/m.K
Density of bottom plate	ρ_b	2700 kg/m^3
Thickness of bottom plate	δ_b	1 mm
Emissivity of bottom plate	ε_b	0.95
Insulation thickness	δ_i	50 mm
Conductivity of insulation	k_i	0.04 W/m.K
Collector length	L	4 m
Collector width	W	1.5 m
Air channel height	H	30 mm
Air velocity	V	1.72 m/s
Wind velocity	V_W	1.5 m/s
Time step	Δt	2 s
Spatial step	Δx	0.05 m

The air temperature exiting collector (T_o) with time and mathematical model is shown in Figure 3. There is excellent consistency between models. The temperature profiles of models 1 and 2 are almost identical. The maximum difference of outlet air temperature between model 1 and 2 is 0.18 K. The outlet air temperature of model 3 is insignificantly lower before 13 PM, and insignificantly higher after 13 PM. This is because model 3 considers the thickness of the glass and plates. Hence the effect of heat storage as radiation increases (7 AM to 13 PM) and discharge as radiation decreases (13 PM to 18 PM). The highest air temperature leaving collector is of 45°C at 13 PM. The largest temperature difference between the airflow and the ambient of 23.5 K also occurs at this time.

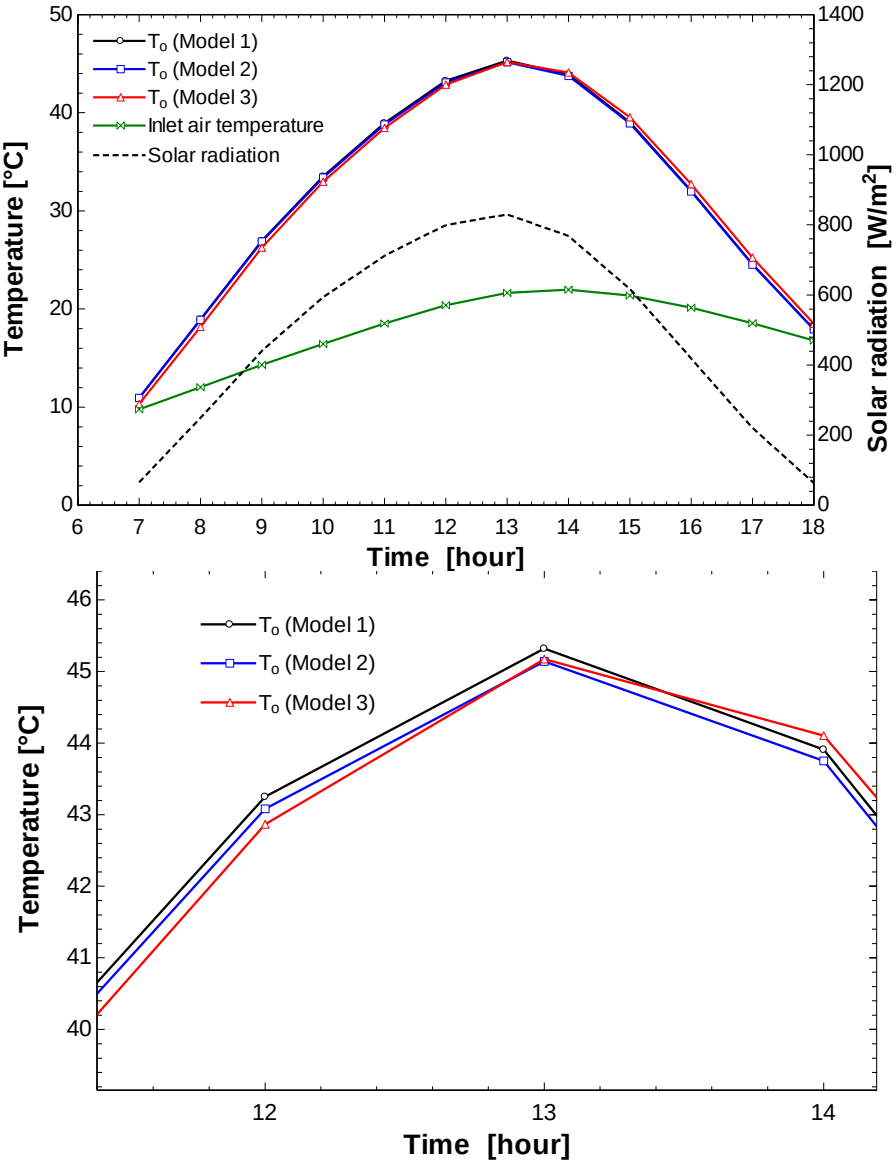

Fig. 3. Variation of outlet air temperature with mathematical models

The variation of the four temperatures along the collector length at 10 AM is shown in Figure 4. There is a good agreement of the air temperature between models 2 and 3 as shown in Figure 4(a). The air temperature profile in model 2 seems to be linear since the second derivative of the air temperature $\left(\frac{\partial^2 T_f}{\partial x^2}\right)$ is not considered in this model. At the entrance segment of the collector (L < 0.4 m), the temperatures of the glass and plates in model 3 are higher than those of model 2. This is because of heat storage of the solids which is considered in model 3. In this first segment, the high temperature of the surfaces causes heat transfer to the inlet air with low temperature so that their temperature is reduced to a minimum at certain location. After this position, the surface temperature increases as the air temperature increases. The bottom plate temperature difference between the two models is greatest as shown in Figure 4(d).

The local temperature predictions of models 2 and 3 are no longer discrepancy when the thickness of the solids is very small as shown in Figure 5 with thickness of 0.02 mm. The coincidence in predicted outlet air temperature (Figure 3) and local temperature (Figure 5) shows that the establishment and solution technique of the 3 models are reasonable. Figure 5 shows that the air

temperature rises more notably than the glass temperature so that the cross temperature occurs at L = 2.2 m. This is because the air receives heat from the absorber and bottom plates.

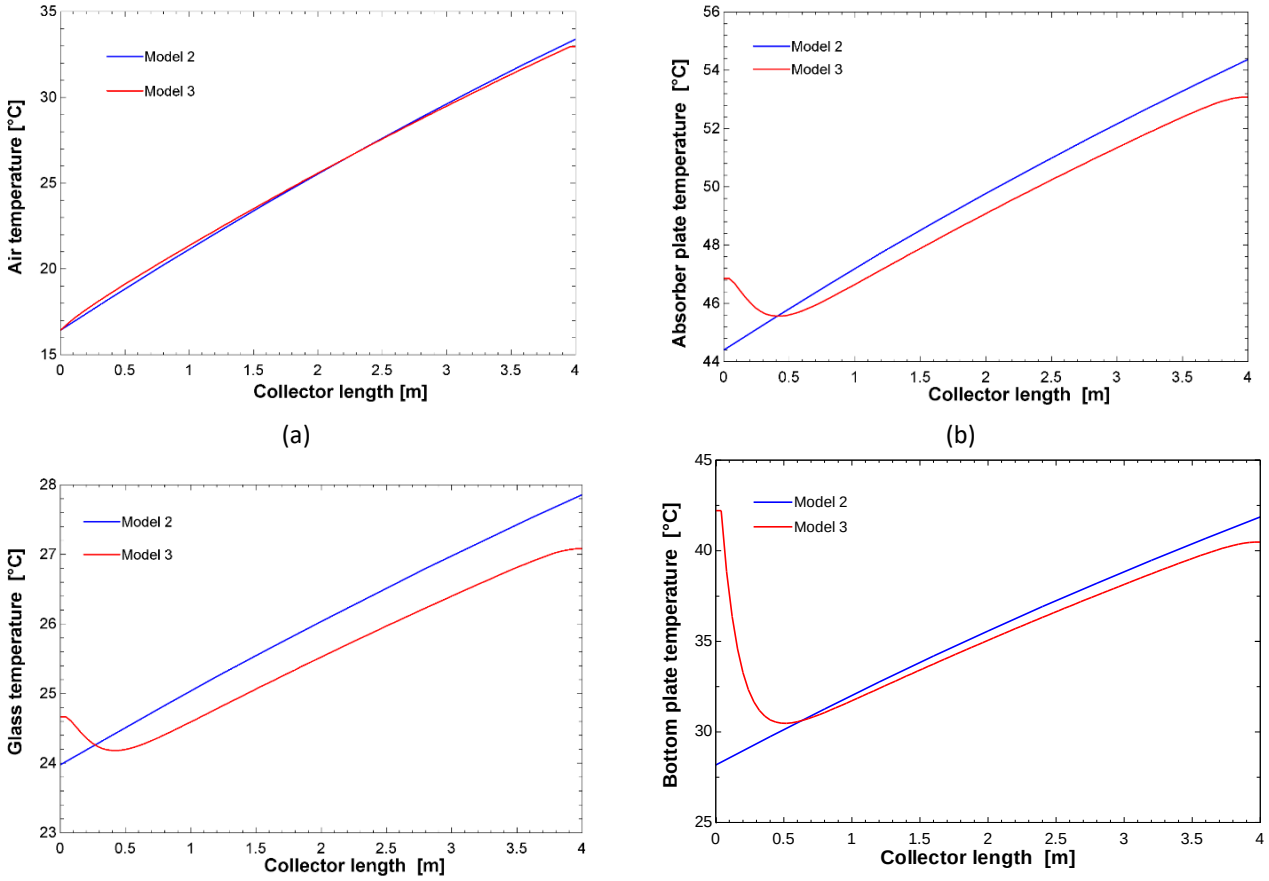

Fig. 4. Local temperatures at 10:00 AM, a) T_f, b) T_p, c) T_g, d) T_b

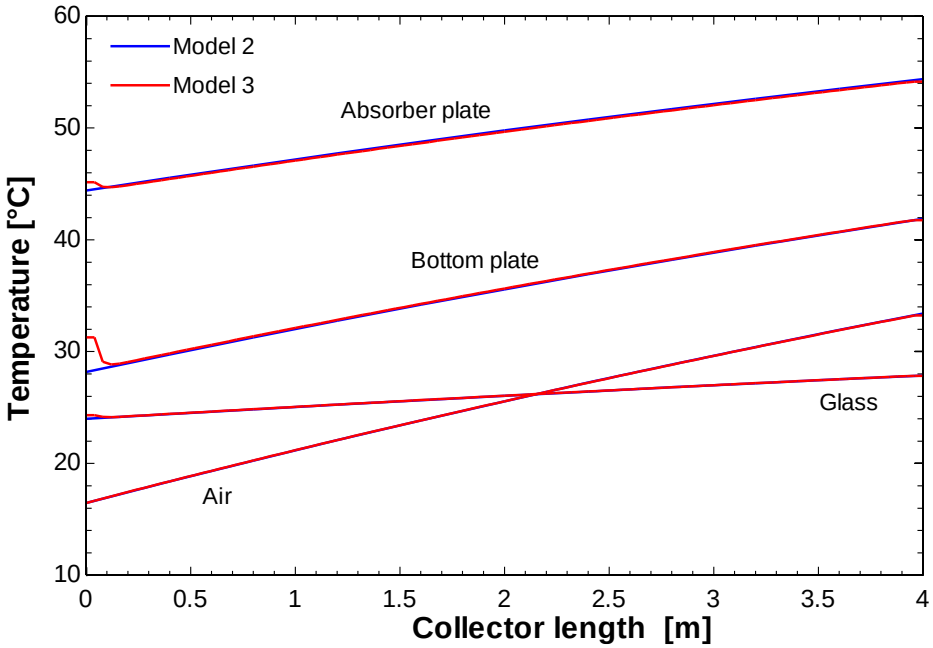

Fig. 5. Local temperatures at 10:00 AM with very thin glass and plates ($\delta_g=\delta_p=\delta_b$= 0.02 mm)

5. Conclusion

In this study, three commonly used mathematical models to predict the operating temperature of the air collector are presented. The complexity of mathematical modeling increases from a system of linear equations (model 1) to ordinary differential equations (model 2), and to system of partial differential equations (model 3). The model formulation and solution technique were successful due to the extreme coincide of the outlet air temperatures. Model 1 predicts outlet air temperature well despite its simple formulation. Models 2 and 3 determine surface temperatures and air in the direction of airflow. Model 3 considers the thickness of the glass, absorber plate, and bottom plate. The important findings are drawn as follows

i. The outlet air temperature prediction is mostly the same among the 3 approaches. The outlet temperature in model 3 is slightly lower and higher in the morning and afternoon, respectively, due to the influence of thermal inertia.
ii. The temperature of glass, absorber plate and bottom plate in model 2 increases with the airflow direction.
iii. The glass, absorber plate, and bottom plate temperatures in model 3 are minimal at certain locations when their thickness is considered. The temperature profiles in model 3 coincide with those of model 2 when the thickness is negligible.

Model 1 can be used for a fast prediction of thermal performance in a practical application. Model 2 can analyze local temperatures to avoid the temperature cross. Model 3 can be expanded to transient SAHs with sensible heat storage by considering the thickness of a plate.

In addition, although a bulk of mathematical modeling publications have been carried out for SAH, further attempts are still required as follows

i. To consider thermophysical properties of air and solids as a function of local temperature.
ii. To examine multidimensional spatial models in conjunction with air pressure distribution
iii. To analytically study sensible and latent heat storage in solar air heaters.

Acknowledgement
This research was not funded by any grant.

References

[1] Benhamza, Abderrahmane, Abdelghani Boubekri, Abdelmalek Atia, Tarik Hadibi, and Müslüm Arıcı. "Drying uniformity analysis of an indirect solar dryer based on computational fluid dynamics and image processing." *Sustainable Energy Technologies and Assessments* 47 (2021): 101466. https://doi.org/10.1016/j.seta.2021.101466

[2] Benhamza, Abderrahmane, Abdelghani Boubekri, Abdelmalek Atia, Hicham El Ferouali, Tarik Hadibi, Müslüm Arıcı, and Naji Abdenouri. "Multi-objective design optimization of solar air heater for food drying based on energy, exergy and improvement potential." *Renewable Energy* 169 (2021): 1190-1209. https://doi.org/10.1016/j.renene.2021.01.086

[3] Phu, Nguyen Minh, and Nguyen Thanh Luan. "A review of energy and exergy analyses of a roughened solar air heater." *Journal of Advanced Research in Fluid Mechanics and Thermal Sciences* 77, no. 2 (2021): 160-175. https://doi.org/10.37934/arfmts.77.2.160175

[4] Minh, Ha Nguyen, and Luan Nguyen Thanh. "The Effective and Exergy Efficiency of Multi-Pass Solar Air Collector with Longitudinal Fins: Analysis and Optimization." *Journal of Advanced Research in Fluid Mechanics and Thermal Sciences* 102, no. 2 (2023): 42-65. https://doi.org/10.37934/arfmts.102.2.4265

[5] Fattoum, Raoua, Ammar Hidouri, Mohammed El Hadi Attia, Müslüm Arıcı, Mohamed Ammar Abbassi, and Zied Driss. "Numerical investigation of influence of the absorber shape on thermal performance of a solar collector." *Journal of Thermal Analysis and Calorimetry* (2022): 1-16. https://doi.org/10.1007/s10973-022-11744-3
[6] Sheikholeslami, M., and Z. Ebrahimpour. "Thermal improvement of linear Fresnel solar system utilizing Al2O3-water nanofluid and multi-way twisted tape." *International Journal of Thermal Sciences* 176 (2022): 107505. https://doi.org/10.1016/j.ijthermalsci.2022.107505
[7] Khalili, Z., and M. Sheikholeslami. "Investigation of innovative cooling system for photovoltaic solar unit in existence of thermoelectric layer utilizing hybrid nanomaterial and Y-shaped fins." *Sustainable Cities and Society* 93 (2023): 104543. https://doi.org/10.1016/j.scs.2023.104543
[8] Phu, Nguyen Minh, Pham Ba Thao, and Duong Cong Truyen. "Heat and fluid flow characteristics of nanofluid in a channel baffled opposite to the heated wall." *CFD Letters* 13, no. 1 (2021): 33-44. https://doi.org/10.37934/cfdl.13.1.3344
[9] Close, D. J. "Solar air heaters for low and moderate temperature applications." *Solar energy* 7, no. 3 (1963): 117-124. https://doi.org/10.1016/0038-092X(63)90037-9
[10] Román, Franz, and Oliver Hensel. "A comparison of steady-state and transient modelling approaches for the performance prediction of solar air heaters." *Energy Conversion and Management: X* 16 (2022): 100327. https://doi.org/10.1016/j.ecmx.2022.100327
[11] El-Refaie, M. F., and M. A. Hashish. "Temperature distributions in the flat-plate collector under actual unsteady insolation." *Applied Mathematical Modelling* 4, no. 3 (1980): 181-186. https://doi.org/10.1016/0307-904X(80)90129-8
[12] Garg, H. P., Ram Chandra, and Usha Rani. "Transient analysis of solar air heaters using a finite difference technique." *International Journal of Energy Research* 5, no. 3 (1981): 243-252. https://doi.org/10.1002/er.4440050305
[13] Garg, H. P., G. Datta, and Ashok Kumar Bhargava. "Performance studies on a finned-air heater." *Energy* 14, no. 2 (1989): 87-92. https://doi.org/10.1016/0360-5442(89)90082-0
[14] Ong, K. S. "Thermal performance of solar air heaters: mathematical model and solution procedure." *Solar energy* 55, no. 2 (1995): 93-109. https://doi.org/10.1016/0038-092X(95)00021-I
[15] Ho, C. D., C. W. Yeh, and S. M. Hsieh. "Improvement in device performance of multi-pass flat-plate solar air heaters with external recycle." *Renewable Energy* 30, no. 10 (2005): 1601-1621. https://doi.org/10.1016/j.renene.2004.11.009
[16] Ramadan, M. R. I., A. A. El-Sebaii, S. Aboul-Enein, and E. El-Bialy. "Thermal performance of a packed bed double-pass solar air heater." *Energy* 32, no. 8 (2007): 1524-1535. https://doi.org/10.1016/j.energy.2006.09.019
[17] Sopian, Kamaruzzaman, M. A. Alghoul, Ebrahim M. Alfegi, M. Y. Sulaiman, and E. A. Musa. "Evaluation of thermal efficiency of double-pass solar collector with porous–nonporous media." *Renewable Energy* 34, no. 3 (2009): 640-645. https://doi.org/10.1016/j.renene.2008.05.027
[18] Ramani, B. M., Akhilesh Gupta, and Ravi Kumar. "Performance of a double pass solar air collector." *Solar energy* 84, no. 11 (2010): 1929-1937. https://doi.org/10.1016/j.solener.2010.07.007
[19] Yeh, Ho-Ming, and Chii-Dong Ho. "Collector efficiency in downward-type internal-recycle solar air heaters with attached fins." *Energies* 6, no. 10 (2013): 5130-5144. https://doi.org/10.3390/en6105130
[20] Hernandez, Alejandro L., and José E. Quiñonez. "Analytical models of thermal performance of solar air heaters of double-parallel flow and double-pass counter flow." *Renewable Energy* 55 (2013): 380-391. https://doi.org/10.1016/j.renene.2012.12.050
[21] Ho, Chii-Dong, Chun-Sheng Lin, Yu-Chuan Chuang, and Chun-Chieh Chao. "Performance improvement of wire mesh packed double-pass solar air heaters with external recycle." *Renewable energy* 57 (2013): 479-489. https://doi.org/10.1016/j.renene.2013.02.005
[22] Karim, M. A., Erond Perez, and Zakaria Mohd Amin. "Mathematical modelling of counter flow v-grove solar air collector." *Renewable energy* 67 (2014): 192-201. https://doi.org/10.1016/j.renene.2013.11.027
[23] Velmurugan, P., and R. Kalaivanan. "Energy and exergy analysis of multi-pass flat plate solar air heater—an analytical approach." *International Journal of Green Energy* 12, no. 8 (2015): 810-820. https://doi.org/10.1080/15435075.2014.888662
[24] Velmurugan, P., and R. Kalaivanan. "Energy and exergy analysis of solar air heaters with varied geometries." *Arabian Journal for Science and Engineering* 40 (2015): 1173-1186. https://doi.org/10.1007/s13369-015-1612-2
[25] Velmurugan, P., and R. Kalaivanan. "Thermal performance studies on multi-pass flat-plate solar air heater with longitudinal fins: An analytical approach." *Arabian Journal for Science and Engineering* 40 (2015): 1141-1150. https://doi.org/10.1007/s13369-015-1573-5

[26] Velmurugan, P., and R. Kalaivanan. "Energy and exergy analysis in double-pass solar air heater." *Sādhanā* 41 (2016): 369-376. https://doi.org/10.1007/s12046-015-0456-5
[27] Singh, Satyender, and Prashant Dhiman. "Analytical and experimental investigations of packed bed solar air heaters under the collective effect of recycle ratio and fractional mass flow rate." *Journal of Energy Storage* 16 (2018): 167-186. https://doi.org/10.1016/j.est.2018.01.003
[28] Ho, Chii-Dong, Hsuan Chang, Ching-Fang Hsiao, and Chien-Chang Huang. "Device performance improvement of recycling double-pass cross-corrugated solar air collectors." *Energies* 11, no. 2 (2018): 338. https://doi.org/10.3390/en11020338
[29] Matheswaran, M. M., T. V. Arjunan, and D. Somasundaram. "Analytical investigation of solar air heater with jet impingement using energy and exergy analysis." *Solar Energy* 161 (2018): 25-37. https://doi.org/10.1016/j.solener.2017.12.036
[30] Matheswaran, M. M., T. V. Arjunan, and D. Somasundaram. "Energetic, exergetic and enviro-economic analysis of parallel pass jet plate solar air heater with artificial roughness." *Journal of Thermal Analysis and Calorimetry* 136 (2019): 5-19. https://doi.org/10.1007/s10973-018-7727-4
[31] Luan, Nguyen Thanh, and Nguyen Minh Phu. "First and second law evaluation of multipass flat-plate solar air collector and optimization using preference selection index method." *Mathematical Problems in Engineering* 2021 (2021): 1-16. https://doi.org/10.1155/2021/5563882
[32] Phu, Nguyen Minh, Nguyen Van Hap, Phan Thanh Nhan, and Huynh Phuoc Hien. "A One-dimensional Analysis and Optimum Air Flow Rate of a Triple-Pass Solar Air Heater." In *2021 24th International Conference on Mechatronics Technology (ICMT)*, pp. 1-5. IEEE, 2021. https://doi.org/10.1109/ICMT53429.2021.9687144
[33] Phu, Nguyen Minh, and Ngo Thien Tu. "One-Dimensional Modeling of Triple-Pass Concentric Tube Heat Exchanger in the Parabolic Trough Solar Air Collector." In *Heat Exchangers*. IntechOpen, 2021.
[34] Phu, Nguyen Minh, Ngo Thien Tu, and Nguyen Van Hap. "Thermohydraulic performance and entropy generation of a triple-pass solar air heater with three inlets." *Energies* 14, no. 19 (2021): 6399. https://doi.org/10.3390/en14196399
[35] Ahmadkhani, Ali, Gholamabbas Sadeghi, and Habibollah Safarzadeh. "An in depth evaluation of matrix, external upstream and downstream recycles on a double pass flat plate solar air heater efficacy." *Thermal Science and Engineering Progress* 21 (2021): 100789. https://doi.org/10.1016/j.tsep.2020.100789
[36] Ho, Chii-Dong, Hsuan Chang, Ching-Fang Hsiao, and Yu-Chen Lin. "Optimizing thermal efficiencies of double-pass cross-corrugated solar air heaters on various configurations with external recycling." *Energies* 14, no. 13 (2021): 4019. https://doi.org/10.3390/en14134019
[37] Van Hap, Nguyen, and Nguyen Minh Phu. "Heat Transfer in Double-Pass Solar Air Heater: Mathematical Models and Solution Strategy." *IntechOpen: London, UK* (2022). https://doi.org/10.5772/intechopen.105133
[38] Nhiem, Tran Quoc, Dang Van Hai, Huynh Van Nam, Nguyen Minh Huy, Le The Truyen, and Nguyen Minh Phu. "Comparative Research on Double-Duct and Double-Pass Solar Air Collectors." In *Computational Intelligence Methods for Green Technology and Sustainable Development: Proceedings of the International Conference GTSD2022*, pp. 638-646. Cham: Springer International Publishing, 2022. https://doi.org/10.1007/978-3-031-19694-2_56
[39] Thao, Pham Ba, Duong Cong Truyen, and Nguyen Minh Phu. "Theoretical Prediction of Quadruple-Pass Solar Air Heater with Longitudinal Fins by a One-Dimensional Approach." In *Applied Mechanics and Materials*, vol. 907, pp. 69-77. Trans Tech Publications Ltd, 2022. https://doi.org/10.4028/p-y96ek6
[40] Nellis, Gregory, and Sanford Klein. *Heat transfer*. Cambridge university press, 2008. https://doi.org/10.1017/CBO9780511841606
[41] Tchinda, Réné. "A review of the mathematical models for predicting solar air heaters systems." *Renewable and sustainable energy reviews* 13, no. 8 (2009): 1734-1759. https://doi.org/10.1016/j.rser.2009.01.008